JACS
JOURNAL OF THE AMERICAN CHEMICAL SOCIETY
Article
pubs.acs.org/JACS

Superior Photoprotective Motifs and Mechanisms in Eumelanins Uncovered

Alice Corani,[†] Annemarie Huijser,[†,⊥] Thomas Gustavsson,[‡] Dimitra Markovitsi,[‡] Per-Åke Malmqvist,[§] Alessandro Pezzella,[∥] Marco d'Ischia,[∥] and Villy Sundström*[,†]

[†]Department of Chemical Physics, Lund University, Box 124, 22100 Lund, Sweden
[‡]CNRS, IRAMIS, LIDYL, Laboratoire Francis Perrin, URA 2453, F-91191 Gif-sur-Yvette, France
[§]Division of Theoretical Chemistry, Lund University, Box 124, 22100 Lund, Sweden
[∥]Department of Chemistry Sciences, University of Naples Federico II Via Cintia, 80126 Naples, Italy

Supporting Information

ABSTRACT: Human pigmentation is a complex phenomenon commonly believed to serve a photoprotective function through the generation and strategic localization of black insoluble eumelanin biopolymers in sun exposed areas of the body. Despite compelling biomedical relevance to skin cancer and melanoma, eumelanin photoprotection is still an enigma: What makes this pigment so efficient in dissipating the excess energy brought by harmful UV-light as heat? Why has Nature selected 5,6-dihydroxyindole-2-carboxylic acid (DHICA) as the major building block of the pigment instead of the decarboxylated derivative (DHI)? By using pico- and femtosecond fluorescence spectroscopy we demonstrate herein that the excited state deactivation in DHICA oligomers is 3 orders of magnitude faster compared to DHI oligomers. This drastic effect is attributed to their specific structural patterns enabling multiple pathways of intra- and interunit proton transfer. The discovery that DHICA-based scaffolds specifically confer uniquely robust photoprotective properties to natural eumelanins settles a fundamental gap in the biology of human pigmentation and opens the doorway to attractive advances and applications.

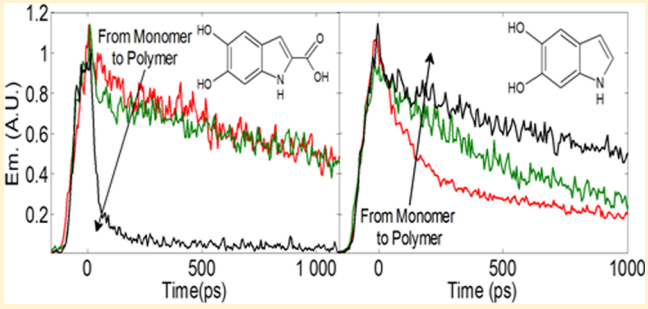

INTRODUCTION

Melanins are a class of biopolymers responsible for the pigmentation of the human skin, hair, and eyes.[1] Epidermal pigments can be divided into two classes: the black to brown eumelanins and the yellow to reddish pheomelanins. The former are mainly responsible for the pigmentation of darker skin types while the latter are typically found in the skins of redheads with freckles and a fair complexion. Both types of melanins are synthesized in the melanocytes via tyrosinase-catalyzed oxidation of tyrosine into dopaquinone. In the eumelanin forming pathway dopaquinone is converted to dopachrome which rearranges with or without decarboxylation to give the ultimate monomer precursors 5,6-dihydroxyindole (DHI) and 5,6-dihydroxyindole-2-carboxylic acid (DHICA) (Figure 1). Oxidative polymerization of the latter accounts for the deposition of black insoluble eumelanin pigments. When chemically produced in vitro, eumelanins consist mainly, if not solely, of DHI-derived oligomer/polymer species reflecting the tendency of dopachrome to undergo rearrangement with spontaneous decarboxylation.[2] In vivo, however, dopachrome rearrangement is regulated by the enzyme dopachrome tautomerase or tyrosinase-related protein 2 (Tyrp-2), which promotes the alternate nondecarboxylative pathway leading to the formation of DHICA. The actual role and significance of Tyrp-2 is still obscure, although new data would suggest a central role of DHICA in reinforcing the antioxidant properties of eumelanins[3] and in serving as an antioxidant,[4] antiproliferative, protective, and antiapoptotic endogenous cell messenger playing a central role in skin homeostasis.[5] Whether and to what extent enzyme controlled incorporation of DHICA, rather than the more oxidizable and pigmentogenic DHI, into natural eumelanins has any functional significance in human photoprotection is an unresolved enigma.

Both natural and synthetic eumelanins show a broad absorption profile with decreasing intensity from the UV to visible region.[6] This is generally attributed to a largely heterogeneous chemical composition and can be modeled by a superposition of a large number of inhomogeneously broadened transitions associated with the individual segments in the pigment.[6−9] The coexistence of both reduced and oxidized domains favoring aggregation of polymer chains and intermolecular chromophore perturbation has also been implicated to account for the featureless visible absorption spectrum of eumelanins.[10,11]

Received: February 12, 2014
Published: July 31, 2014

   dx.doi.org/10.1021/ja501499q | J. Am. Chem. Soc. 2014, 136, 11626−11635

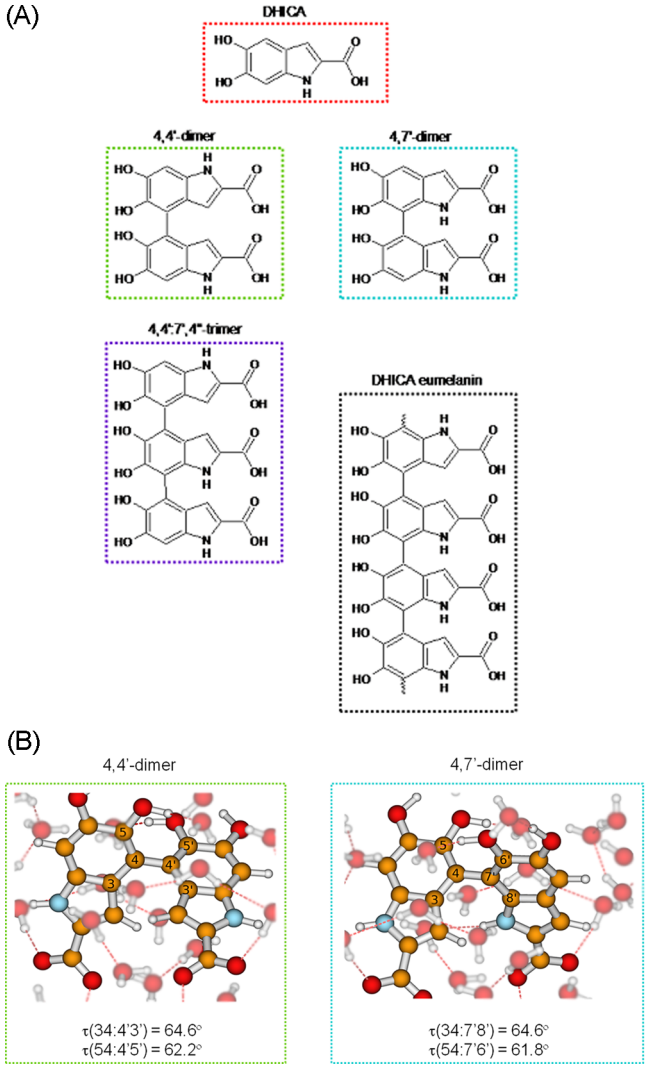

Figure 1. (A) Formulas showing DHICA, the 4,4′- and 4,7′-dimers, and the polymer (representative model structure). (B) Calculated ground state geometries of the 4,4′- and 4,7′-dimers in H_2O, with the torsion angles between the DHICA units indicated.

Eumelanin is known to possess very efficient (99.9%) dissipation channels of absorbed UV energy into heat, but despite many spectroscopic studies the mechanisms of this very efficient photoprotection are not known.[12−17] In particular, the minimum functional units and active photochemical processes associated with the efficient UV energy dissipation are unknown. As a straightforward approach to settle these issues, we have recently undertaken a systematic bottom-up investigation by comparing the excited state dynamics of key eumelanin building blocks and model systems from the monomer through the dimer and oligomer to the homopolymer stage. Using the previously studied DHICA photochemistry as a starting point,[18−20] and taking the results of studies on DHI and its oligomers[21] as a basis for comparison, we report herein an investigation on the excited state deactivation mechanisms of isomeric DHICA dimers (with the 4,4′- and the 4,7′-*inter*-unit bonding pattern), trimer (4,4′:7′,4″-bonding), and polymer (Figure 1).[22] Excited state dynamics are studied by time-resolved fluorescence using fs UV excitation in combination with fluorescence up-conversion (FU) and streak camera (SC) detection.

RESULTS

Sample Preparation and Experiment Design. DHICA melanin is poorly soluble in aqueous buffer but could be obtained in a water-soluble form by oxidative polymerization of DHICA in phosphate buffer containing poly(vinyl alcohol) (PVA).[23] Under such conditions, the DHICA melanin structure would not be affected by PVA, since no evidence was previously obtained for a direct chemical interaction between the polymer and the developing melanin.[23] In line with this conclusion, precipitation of native melanin occurs by simple dilution of the PVA solution with PVA-free buffer. DHICA possesses three acidic groups; the carboxyl group at C-2 and the two hydroxyl groups at C-6 and C-5. The pK_a values for these groups are 4.25, 9.76, and 13.2, respectively.[24,25] Assuming that these values do not change significantly upon covalent bonding of DHICA monomers, it can be inferred that under moderately acidic conditions the hydroxyl groups are fully protonated, but the carboxylic acid groups could be partially deprotonated. To address the influence of the protonation state of the carboxylic acid group on excited state deactivation, we performed studies at both acidic and neutral conditions. At pH 2.5 the fully protonated carboxylic acid group is by far the prevalent form, while the deprotonated carboxylate anion is the only relevant state (>99%) at pH 7.0. Concentrations in the range 0.1−0.5 mM were used, depending on the fluorescence techniques, the excitation wavelength, and the solvent used. Concentrations were calculated from the absorption spectrum, using the extinction coefficient in ethanol given in ref 26.

Steady-State Optical Characteristics. DHICA and DHICA-based model compounds, namely the 4,4′- and 4,7′-dimers, the 4,4′:7′,4″-trimer, and the polymer obtained by oxidation of DHICA under biomimetic conditions were investigated (Figure 1A). Details regarding sample preparation are described in the Methods section. Figure 2 shows the

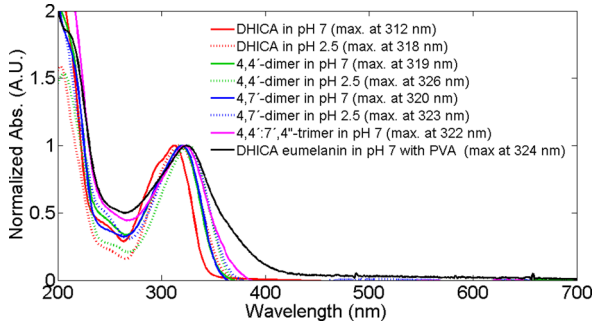

Figure 2. Normalized absorption spectra of the DHICA monomer in pH 7.0 and pH 2.5 buffer, the 4,4′- and 4,7′-dimers in pH 7.0 and pH 2.5 buffers, and the DHICA eumelanin pigment in pH 7.0 buffer solubilized using less than 1% (by weight) PVA.

absorption spectra of the samples studied at pH 2.5 and pH 7. A close similarity of these spectra with the spectrum of a DHICA-containing natural melanin[27] is apparent. Upon deprotonation of the carboxyl groups (pH 7) there is an approximately 6 nm blue shift in the maximum of the monomer spectrum, which becomes somewhat smaller (3−6 nm) for the oligomers. This spectral shift was very recently observed also for indole-2-carboxylic acid (ICA) and explained with the help of quantum chemistry calculations as a result of decreased oscillator strength of the lowest S_0-S_1 transition upon COOH-group deprotonation.[28] Dimers exhibit a red shift of 5−8 nm

dx.doi.org/10.1021/ja501499q | J. Am. Chem. Soc. 2014, 136, 11626−11635

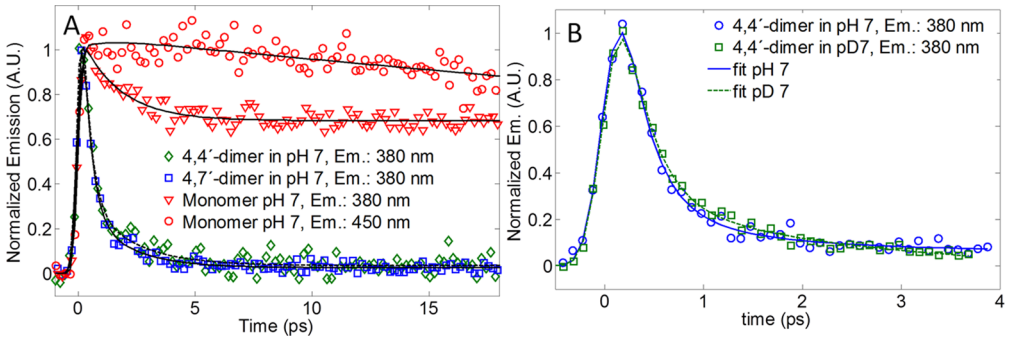

Figure 3. Fluorescence up-conversion decays obtained for (A) DHICA monomer and 4,4′- and 4,7′-dimers (the ∼1 ps decay at 380 nm and corresponding weak rise at 450 nm of the monomer DHICA$^-$ kinetics is due to excited state solvation dynamics[20,83]) and (B) deuterated 4,4′- and 4,7′-dimers. Excitation wavelength: 267 nm.

Table 1. Lifetimes Obtained by Fitting the Up-Conversion Data[a]

	pH 2.5		pH 7		MeOH	
	decay time (ps)	amplitude	decay time (ps)	amplitude	decay time (ps)	amplitude
monomer	1600 ± 150	0.09	1600 ± 150	0.62	3500 ± 300	0.29
	1.10 ± 0.15	0.33	1.10 ± 0.15	0.38	10.70 ± 1.10	0.71
	0.30 ± 0.10	0.59				
4,4′-dimer	1600 ± 150	0.03	1600 ± 150	0.04	3500 ± 300	0.02
	1.10 ± 0.15	0.05	1.10 ± 0.15	0.14	10.70 ± 1.10	0.27
	0.19 ± 0.09	0.92	0.26 ± 0.10	0.83	0.70 ± 0.20	0.71
4,7′-dimer	1600 ± 150	0.01	1600 ± 150	0.02	3500 ± 300	0.01
	1.10 ± 0.15	0.14	1.10 ± 0.15	0.25	10.70 ± 1.10	0.33
	0.19 ± 0.10	0.85	0.31 ± 0.11	0.74	0.70 ± 0.20	0.66

[a]The response function FWHM is fixed at 346 fs, and lifetimes larger than 20 ps are fixed as obtained from the streak camera experiments.

of the absorption maxima relative the DHICA monomer at both pH values, and the trimer has a shift of 10 nm at pH 7. These shifts have been previously reported[29] and could in principle be taken to indicate a certain degree of electron delocalization or excitonic interaction between monomer units in DHICA oligomers. In the case of exciton (dipole−dipole) interaction, the delocalized excited state could be imagined to give rise to ultrafast dynamics due to exciton relaxation and localization. As we will argue below, due to the basically sandwich type of relative orientation of the monomeric units and their transition dipoles (H-aggregate) (Figure 1 B) any dipole−dipole interaction is expected to lead to a blue shift of oligomer absorption spectra. It is therefore highly unlikely that dipole−dipole interaction is the origin of the red shift of dimer and trimer absorption spectra (more below, Discussion), and we conclude that optical excitation of DHICA oligomers results in localized excited states.

The absorption spectrum of the DHICA synthetic polymer shows significant resemblance with those of the dimers, although it exhibits in addition the typical eumelanin-like featureless absorption profile in the visible part of the spectrum. The latter is likely due to both intrinsic and extrinsic components reflecting intramolecular electron delocalization between oxidized (quinonoid) and reduced (catechol) moieties and intermolecular chromophore perturbation effects. The absorption maximum in the UV region is largely due to monomer-like behavior.

Excited-State Dynamics. We start by considering the excited state dynamics of the dimer and trimer molecules at pH 7 where the deprotonated carboxylate anion is the dominating state. Figure 3 shows the FU decays of the 4,4′- and 4,7′-dimers and for comparison the corresponding kinetics of the DHICA monomer. Upon covalent bonding of the DHICA monomers into dimers the excited state lifetime drastically shortens from ∼1.6 ns[18,20,30] to ∼300 fs. Approximately 90% of the fluorescence decay amplitude is accounted for by this subps component and only <10% by slower ps and ns components (Table 1). SC measurements of carefully purified samples showed that the amplitude of this slow decay is further decreased by approximately a factor of 10 to less than 1% of the total amplitude. This low intensity slow background decay represents the noise level due to very small residual amounts of the DHICA$^-$ monomer anion. Clearly, 4,4′- or 4,7′- covalent bonding into a dimer opens up a subps decay channel that is not accessible to the DHICA monomer carboxylate anion. The similar kinetics for the 4,4′- and 4,7′-dimers demonstrate that this excited-state relaxation process occurs in both dimers and is not significantly affected by the bonding pattern and coupling positions. SC measurements were performed on the dimers at many more wavelengths across the fluorescence spectrum. The ∼5 ps resolution of the streak camera does not allow us to resolve the subps decay, but the amplitude of this decay is a sensitive marker of the lifetime. A wavelength dependence of the amplitudes that mirrors the fluorescence spectrum suggests that there is no significant wavelength dependence of the subps decay (see SI Figure SI1A, B).

Only SC measurements with lower time resolution (∼5 ps) were performed on the trimer carboxylate anion (see SI, Figure SI2). Obviously the lower time resolution of the streak camera is not capable of resolving the very fast subps decays of the oligomers. Nevertheless, the amplitude−lifetime relation of an unresolved decay mentioned above and the fact that the very short-lived fluorescence can still be detected for all three oligomers with similar peak intensity suggest that they all are of comparable lifetimes. The somewhat lower peak fluorescence

dx.doi.org/10.1021/ja501499q | J. Am. Chem. Soc. 2014, 136, 11626−11635

intensity of the trimer probably implies that its excited state lifetime is even shorter than the ∼300 fs of the dimers.

The fluorescence kinetics of the 4,4′- and 4,7′-dimers in pH 2.5 buffer, in which the carboxylic acid groups are virtually completely protonated, are shown in Figure 4 A. Both dimers

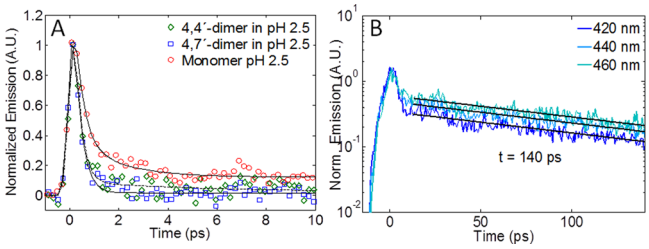

Figure 4. (A) Fluorescence up-conversion decays at 380 nm of the fully protonated DHICA 4,4′- and 4,7′-dimers at pH 2.5. The monomer decay at the same pH is shown for comparison.[20] (B) Streak camera fluorescence decays of the fully protonated 4,4′- and 4,7′-dimers at pH 2.5. Excitation wavelength 267 nm.

have very similar decays dominated by an ultrafast ∼190 fs lifetime, i.e. almost a factor of 2 faster decay than that for the protonated DHICA monomer[20] (kinetics also shown in Figure 4A for comparison), or the deprotonated dimers (Figure 3). The fluorescence decays of the fully protonated dimers were also measured with the streak camera at several detection wavelengths (Figure SI3A and B). Despite the lower time resolution of the streak camera, the subps decay of the dimers is detected as a response limited decay in the blue part (λ < 400 nm) of the fluorescence spectrum. At longer wavelengths (> 420 nm), a slower ∼140 ps fluorescence decay, reminiscent of the red-shifted zwitterionic fluorescence observed for the DHICA monomer, becomes apparent (Figure 4B).

We showed previously that the DHICA monomer fluorescence decay is very sensitive to the nature of the solvent and becomes very long (∼3.5 ns) in methanol.[20] Figure 5

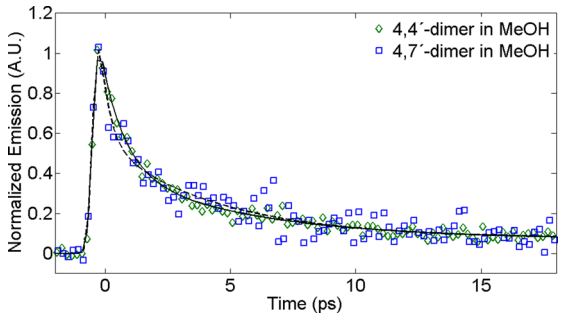

Figure 5. Fluorescence up-conversion decays at 380 nm of DHICA 4,4′- and 4,7′-dimers in MeOH. Excitation wavelength 267 nm.

shows fluorescence kinetics of the 4,4′- and 4,7′-dimers in methanol. We can see that the fluorescence decays of the dimers become much slower in methanol than in the buffer solution; an exponential fit results in two lifetimes of about 1 and 10 ps, and the average 1/e lifetime, 3−4 ps, is approximately a factor of 10 slower than that in aqueous buffer solution.

For identifying a possible minimal functional unit of eumelanin in UV-dissipation, a comparison between oligomer and polymer excited state decay is important. The fluorescence decay of the synthetic DHICA polymer at pH 7 in PVA/buffer solution (Figure 6) exhibits an ultrafast subps decay (∼160 fs),

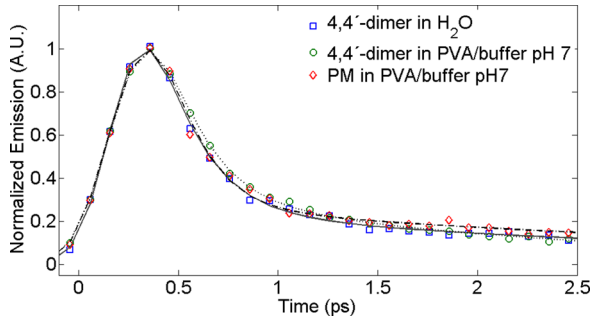

Figure 6. Fluorescence up-conversion decays at 380 nm of the DHICA 4,4′-dimer in aqueous and PVA solution, and DHICA polymer (PM) solubilized in PVA/buffer solution. Excitation wavelength 267 nm.

similar and perhaps even faster than that of the dimers. This shows that the very efficient excited state deactivation process dealt with here is already active in the dimer and does not evolve much further when going to the trimer and polymer.

Solvent mediated excited state proton transfer (ESPT) was shown to be responsible for the DHICA monomer excited state dynamics.[20] With that in mind the kinetic deuterium isotope effect of the 4,4′-dimer anion in aqueous buffer solution was measured. A kinetic isotope effect (KIE = ratio between proton transfer rates of the hydrogenated and the deuterated molecules) is traditionally seen as evidence for a tunneling mechanism of proton transfer, and it is postulated that the KIE approaches the square-root of two (∼1.4) for very fast transfer.[31−33] The fastest ESPT processes reported exhibit KIEs in the range of 1.4−1.7,[31,34−36] and excited state intramolecular proton transfer (ESIPT) processes have in certain cases been reported to be insensitive to deuteration.[37−39] The fluorescence kinetics in Figure 3B show that the excited state lifetime becomes somewhat longer upon deuteration, 290 fs as compared to 260 fs for the hydrogenated form (Table 2), corresponding to a very small kinetic isotope effect KIE = 1.1 ± 0.5. This near lack of a kinetic isotope effect has only been observed for ultrafast ESIPT processes (see also Discussion).

DISCUSSION

In the case of the monomeric DHICA excited state, the neutral fully protonated form converts to a zwitterion in 300 fs, which then returns to the ground state with a 240 ps time constant,[20] whereas the anion form converts only slowly on the nanosecond time scale to the dianion through excited state proton transfer to the solvent; this dianion has a long (2.4 ns) excited state lifetime.[20] Thus, monomeric DHICA has a limited excited state energy dissipation capability, via the relatively short lifetime of its zwitterionic form.[19,30] For the dimeric and oligomeric forms the situation is dramatically different; all forms have an extremely efficient dissipation of excited state energy, at least 1000-fold more than that of monomeric DHICA. The above results show that covalent bonding of DHICA units into oligomeric or polymeric scaffolds introduces pathways for ultrafast excited-state deactivation unavailable to the monomer. The similar dynamics observed for the 4,4′- and 4,7′-dimers strongly suggest that the mode of bonding does not significantly affect the excited-state processes. However, the excited-state deactivation rate was found to increase in the fully protonated molecules (pH 2.5). In view of the structural features carried by the DHICA oligomers (multiple functional groups with proton donor/acceptor properties,[18−20,25,30]

dx.doi.org/10.1021/ja501499q | J. Am. Chem. Soc. 2014, 136, 11626−11635

Table 2. Fluorescence Lifetimes of Deuturated Dimer and the DHICA Polymer[a]

4,4′-dimer in pH 7	decay time	1600 ± 150 ps	1.10 ± 0.15 ps	0.26 ± 0.10 ps
	amplitude	0.04	0.14	0.83
4,4′-dimer in D_2O	decay time	2300 ± 150 ps	2.40 ± 0.23 ps	0.29 ± 0.15 ps
	amplitude	0.01	0.14	0.89
DHICA Polymer in PVA/buffer	decay time	1600 ± 150 ps	1.30 ± 0.17 ps	0.16 ± 0.09 ps
	amplitude	0.05	0.14	0.81

[a]The response function FWHM is fixed at 346 fs, and lifetimes larger than 20 ps are fixed as obtained from the streak camera experiments.

modest conformational flexibility, and closely spaced chromophores) we are considering three different mechanisms for the observed ultrafast excited state relaxations: (i) conformational dynamics; (ii) exciton relaxation and localization; and (iii) excited state proton transfer. These deliberations lead to the conclusion that the very efficient nonradiative excited state deactivation is a result of fast solvent-assisted excited state proton transfer within and between DHICA units of an oligomeric structure.

Conformational or Exciton Dynamics As Excited State Dissipation Mechanisms? Various flexible molecules such as, e.g., *trans*-and *cis*-stilbene,[40,41] cyanine dyes,[42,43] or triphenyl methane dyes[44] are known to have efficient excited state deactivation through excited state isomerization or conformational changes. Since such processes are characterized by large conformational changes, their rates are generally strongly dependent on the viscosity of the surrounding solvent medium; a higher viscosity leads to a slower reaction. To assess whether the observed very fast excited state decays of the DHICA oligomers could be caused by such structural relaxation processes, we measured the fluorescence decays of the two dimers in a water buffer and methanol. The excited state decay of the DHICA dimers becomes approximately a factor of 10 slower in methanol as compared to aqueous buffer, despite the fact that methanol has a viscosity approximately half that of water (Figure 5, Table 1). This shows that viscosity does not have a noticeable influence on the dimer relaxation dynamics. We believe that these results exclude the possibility of conformational dynamics being the mechanism of excited state deactivation in dimers and oligomers.

Within oligomeric scaffolds, monomeric DHICA units are connected at the 4,4′- or 4,7′-positions via a single bond that brings the individual units quite close together. Therefore, electronic interactions leading to excited state delocalization over more than one DHICA subunit should be considered. Such interaction and exciton state delocalization are well-known phenomena from, e.g., molecular aggregates and photosynthetic antenna pigments and characterized by the appearance of new spectral features corresponding to the upper and lower exciton states.[45−48] Details of these spectral features depend on the strength of interaction and structure of the molecular aggregate. In general it is expected that the lowest exciton state is long-lived and emitting (apart from very special subunit geometries, e.g. strictly sandwich or perfectly circular aggregates[46]) and that population of upper exciton states leads to a very fast relaxation to the lowest states. For the 4,4′- and 4,7′-couplings the dimers and trimers studied here, the DHICA monomers and transition dipoles are in a sandwich configuration, which will result in the upper exciton state being allowed[46,49] and therefore a spectral blue shift relative to the monomer absorption spectrum. According to the ground state geometry calculations (Figure 1 B) the molecular planes of the dimer subunits are at an angle of ∼60°, which would reduce any dipole−dipole interaction to 0.4−0.5 of the value of parallel dipoles. We perform our measurements in low-viscous aqueous and methanol solutions, where the single bond coupling between the monomer units of a dimer is expected to lead to a broad distribution of twist angles from the calculated ∼60°. Through the angle dependence of the exciton level splitting (and spectral shift) we would expect a significant broadening of the oligomeric spectra as compared to the monomer spectra. We do not observe that, but rather a red shift with a more or less maintained spectral shape. From this we conclude that the observed red shift of the oligomer absorption spectra cannot be of excitonic origin, but must be of a different nature. Coupling of several subunits may increase the electron delocalization somewhat, or influence relative oscillator strengths of absorption transitions. Future quantum chemistry calculations will hopefully help resolve this issue. A possible level of dipole−dipole interaction is indicated by the results for aromatic molecules coupled in dimeric structures similar to those of the DHICA dimers;[50,51] an exciton splitting on the order of 10 cm^{-1} had been calculated and measured. Couplings of the same order of magnitude can be expected in the DHICA oligomers. The structural heterogeneity present in solution along with dynamical disorder will by far override such weak couplings and result in localized excited states. From these considerations we conclude that exciton relaxation or localization dynamics within the DHICA oligomers cannot explain our observations.

Excited State Proton Transfer as an Excited State Dissipation Mechanism. Proton transfer from a photoexcited molecule (a photoacid) to the solvent (ESPT) may occur if the excited molecule is a stronger acid than the ground state. A red-shifted absorption or fluorescence spectrum of the conjugate base of the molecule as compared to the acid form is a signature of this.[52] The rates of ESPT vary widely, from nanoseconds to picoseconds depending on the photoacid strength and various solvent properties.[31−33,53−56] If proton donating and accepting groups are situated within the same molecule, an intramolecular excited state proton transfer (ESIPT) may occur. Such proton transfer often occurs along a pre-existing hydrogen bond and therefore becomes very fast, frequently on the ∼100 fs time scale or even faster.[36]

ESPT to solvent has been studied for more than 60 years,[52,57,58] and many theoretical models have been proposed to describe various aspects of the transfer process, e.g. the dependence of transfer kinetics on solvent, temperature, pressure, deuterium substitution, complex formation, etc. The water cluster model of Robinson[55] was an early attempt to explain the solvent dependence of ESPT. More recently, Fleming and Pines[56] related the proton transfer rate to the excited state equilibrium constant, and Huppert and Agmon[53] suggested that the proton transfer is controlled by the number of H-bonds formed and broken. Hynes and co-workers[54] developed a Landau−Zener curve crossing formalism for the ESPT encompassing the range of proton couplings from

nonadiabatic tunneling to solvent controlled regime. The origin of photoacid potential energy surface structures underlying the ESPT process has been addressed by Domcke and Sobolewski;[59−61] based on high level quantum chemistry calculations, conical intersections between excited and ground state surfaces define the reaction path and give rise to ultrafast internal conversion driven by hydrogen detachment in isolated systems, and solute−solvent hydrogen atom transfer in solvent clusters and solution. The role of ESPT for the function of various biological systems has also been extensively studied and discussed,[62−66] and frequently found to be a complex process involving proton transfer chains.[63,65,66]

Dimers, oligomers, and the polymer of DHICA all exhibit ultrafast subps excited state decay at both neutral and acidic pH. We showed above that conformational dynamics and exciton relaxation involving delocalized excited states can be excluded as mechanisms for this ultrafast energy dissipation. We previously showed that a solvent controlled ESIPT is responsible for the ultrafast (∼300 fs) excited state decay of the (protonated, pH 2.5) neutral DHICA monomer and formation of a zwitterionic state with short-lived, ∼240 ps, and red-shifted emission.[18,20,30] With this in mind, it could be expected that also the fully protonated (pH 2.5) dimers (and oligomers) exhibit very fast ESIPT and excited state decay as is in fact demonstrated by the ∼190 fs fluorescence decay (Figure 4). The fact that the red-shifted (>420 nm) fluorescence characteristic of the zwitterionic species is observed also for the dimers (Figures 4B and SI3A) is direct evidence for the COOH → NH process.[18,20,30] FU now shows that ESIPT occurs with an ∼190 fs time constant in fully protonated DHICA dimers (see more below), and streak camera measurements (Figure 4B) show that the zwitterionic proton transfer product decays with an ∼140 ps time constant, somewhat faster than the corresponding monomer decay.

FU measurements show that also the DHICA dimer anion, with the carboxyl groups deprotonated, exhibits a subps (300 fs) excited state decay (Figure 3). This is more than a factor of 1000 faster than the 1.6 ns decay of the DHICA monomer anion, due to excited state proton transfer to the solvent (ESPT), involving the 5- and 6-OH groups of $DHICA^-$.[20] We now propose that this intrinsic ESPT property of the OH-functionalities of DHICA is also active for the DHICA dimer anion (as well as oligomer and polymer) and dramatically accelerated through the combined proton accepting capacity of the several OH-groups of a DHICA oligomer and water solvent molecules. The fact that this process only appears upon covalent bonding of two or more DHICA units shows that it has an intersegment origin (not related to conformational or exciton dynamics, as shown above). Similarly to the ESPT process of $DHICA^-$, it has a strong solvent dependence and becomes approximately a factor of 10 slower in methanol, showing that the solvent environment (but not viscosity) is crucial for the rate. We suggest that the difference in hydrogen bonding capacity of water and methanol is the reason for this difference. We believe that these observations taken together are strong arguments for a solvent mediated excited state proton transfer process involving the 5- and 6-OH-groups of two or more DHICA segments of an oligomer. We suggest a picture similar to that proposed to explain the solvent dependence of the COOH-NH ESIPT process of the DHICA monomer[20] and indicated by quantum chemistry calculations of ICA−water complexes.[28] Water molecules are envisaged to take an active part in the transfer as in the model of Tolbert et al.,[52,67] suggesting a proton accepting network formed by solvent molecules and OH substituents, or the solvent wire model of Leutwyler et al.[68,69] Intermolecular ESPT involving proton transfer chains has also been extensively studied and discussed for various biological systems such as GFP.[64−66] Here, in the case of DHICA dimers and oligomers we suggest that the several OH-groups of the DHICA oligomers and surrounding solvent molecules define a pre-existing network of hydrogen bond acceptors along which the expelled proton can be transferred and solvated. This would also explain the high rate of proton transfer in aqueous solution and the approximately ten times slower rate in methanol; in the well-developed aqueous hydrogen bonding network minimal solvent rearrangements would be needed for efficient proton transfer to occur, whereas more extensive and therefore slow reorganization is required in the less-developed hydrogen bonding network of methanol. Based on a comparison with the fluorescence lifetime of the anionic form of the closely related ICA molecule, lacking the 5- and 6-OH groups, it can be concluded that the time constant of proton transfer involving the 5-,6-OH groups of the DHICA monomer slows down from ∼2.5 ns in aqueous solution to at least 16 ns in methanol. This slightly smaller degree of retardation as compared to the dimer could be due to a difference in the H-bonding network caused by the several intramolecular OH-groups of the DHICA oligomers.

For the $DHICA^-$ monomer, the proton transfer product is the $DHICA^{2-}$ dianion (COO^- and O^-) having a red-shifted fluorescence (λ_{max} = 416 nm) with a long lifetime, ∼2.4 ns.[19,20] For the oligomers no such fluorescence is observed above the noise level defined by fluorescence from remaining very low impurity concentrations of monomeric $DHICA^-$ with a fluorescence lifetime of 1.6 ns. This can be explained if the proton transfer product is formed directly in the ground state, or if the PT product excited state decays to the ground state through a very fast internal conversion (IC). In any case, the proton transfer ground state product must be very short-lived since the high repetition rate of the laser excitation pulses (80 MHz, or 12 ns pulse separation) does not cause a significant buildup of photoproduct; a photoproduct lifetime of <1 ns is required to avoid establishment of a photostationary state with most of the molecules in the product state. The H-bond network or solvent wire discussed above would provide the necessary conditions for proton caging. Thus, the several OH-groups of an oligomer together with solvent water molecules provide a proton caging network that not only accelerates the forward proton transfer but also leads to fast back proton transfer to regenerate the original ground state. Such nonradiative excited state quenching by nonadiabatic geminate proton recombination has already been reported for 1-naphthol.[70,71]

In order to obtain additional support for the involvement of the 5- and 6-OH protons of DHICA oligomers in the excited state relaxation process we measured steady state fluorescence spectra of a highly purified sample of the 4,4′-dimer in MeOH and in 0.1 M NaOH (pH 13) (Figure SI4). In MeOH solution we observe a fluorescence band at ∼350 nm, reminiscent of that for monomeric DHICA in MeOH.[20] In strongly alkaline aqueous solution (pH 13) the dimer is expected to exist in a form with one or both of the OH-groups deprotonated, corresponding to the di- or trianions of the DHICA monomer. For weakly interacting DHICA subunits in the dimer, one would expect a fluorescence similar to that of $DHICA^{2-}$ or $DHICA^{3-}$, i.e. red-shifted relative to the fluorescence in MeOH, to 416 nm for the dianion and even more to the red for the trianion.[20] The fluorescence spectrum of the 4,4′-dimer in 0.1 M NaOH (Figure SI4) is in fact characterized by a relatively

dx.doi.org/10.1021/ja501499q | J. Am. Chem. Soc. 2014, 136, 11626−11635

weak band at approximately this wavelength (λ_{max} ~420 nm; already for monomeric DHICA the fluorescence was observed to be weak at pH 13 due to weakly emitting $DHICA^{2-}$ and $DHICA^{3-}$). We believe this is strong evidence for the involvement of the OH protons in the excited state deactivation of anionic DHICA oligomers (carboxyl groups deprotonated and OH groups protonated). In other words, with the OH groups fully protonated ultrafast ESPT occurs which quenches the excited state in 300 fs to such an extent that no steady-state fluorescence can be detected above the noise level; on the other hand, in alkaline solution with the OH groups deprotonated no ESPT can occur and fluorescence that is characteristic of $DHICA^{2-}$ and $DHICA^{3-}$ is observed.

The observed rates of excited state proton transfer for the two channels discussed above, i.e. involving the COOH−NH donor−acceptor pair and the OH-functionalities, ~$(300\ fs)^{-1}$ in oligomers and polymer of DHICA, approach the fastest measured ESPT rates of super photoacids.[31,36,72] For such molecules, subps proton transfer has been observed, with a transfer of ~100 fs, reported to be the fastest to date.[36] In that work, Huppert and co-workers asked the question "how fast can ESPT to solvent get?" and, based on theoretical considerations involving transition state theory or the tunneling mechanism for ESPT,[73−75] suggested that an upper limit may be the very high rates of ~10^{13} s^{-1} reported for ESIPT processes where little solvent reorganization is needed for the transfer to occur. Actually, in the case of a barrierless ESPT reaction, it has been suggested that the characteristic time could be as fast as the OH (OD) stretching vibration period of 30 (50) fs[39] which is below our time resolution. For the fastest ESPT processes, observed KIEs of ~1.4−1.7 have been reported.[31,34−36] The small KIE = 1.1 ± 0.5 obtained for DHICA dimers (pH 7) lies in this range, but the large uncertainty does not allow a more detailed comparison. However, the average value 1.1 is more reminiscent of the lack of a kinetic isotope effect obsreved for very fast ESIPT processes[37−39] which are practically barrierless. The OH-groups of the DHICA oligomers could, together with a water molecule, form an interunit H-bond network which provides the structural features for ESPT with very little solvent molecule reorganization and therefore a small KIE.

The scheme in Figure 7 illustrates the excited state proton transfer processes discussed for oligomeric DHICA. Two distinct pathways are highlighted, namely the intraunit and interunit processes, with the latter occurring only from the dimer level and beyond. One channel involves solvent mediated ESIPT between the COOH and NH functionalities of the neutral molecules with the carboxyl groups protonated. Our experiments unambiguously identify the intermediate species in this process and show that the ESIPT step occurs with an ~$(300\ fs)^{-1}$ rate constant to form a zwitterionic intermediate species that returns to ground state in ~140 ps. The second channel is equally fast resulting in an ~300 fs excited state decay of anionic dimers and polymers (COOH deprotonated) and an overall excited state decay of less than 200 fs of neutral DHICA dimers and polymers where both decay channels are operating. By excluding conformational dynamics and exciton relaxation as mechanisms for the excited state decay we propose that this second channel, exhibiting a strong solvent dependence, dependence on the protonation state of the 5- and 6-OH groups, and small kinetic isotope effect, is an ESPT involving the H-bonding network formed by several OH-groups of the DHICA oligomers and solvent water molecules. The lack of

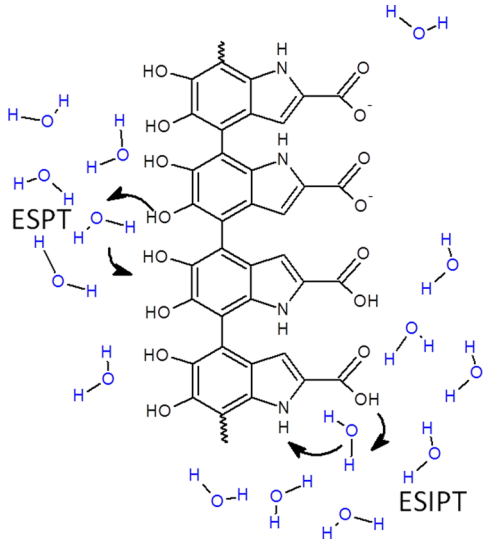

Figure 7. Summary of ultrafast excited state deactivation of DHICA oligomer excited states via competing sub−ps Excited State Proton Transfer (ESPT) processes. Intra- and interunit deactivation channels are highlighted for conditions reflecting the melanin pigment[81] where the ratio of carboxyl and carboxylate is close to 1, i.e. pH ~4.5.

detectable excited state proton transfer product and short-lived ground state product is taken as an indication of the product being formed directly in the ground state, or that the excited state proton transfer product undergoes ultrafast IC to the ground state followed by a fast proton back transfer facilitated by the H-bonding network. The definitive confirmation and further details of the reaction mechanism of this second pathway have to await high-level quantum chemistry and MD calculations to explore the potential energy landscape and dynamics of these complex molecules. Additional experiments aiming at identifying reaction intermediates are also needed. However, the photoprotective function of eumelanin, which is now shown to rely to a significant extent on processes having an interunit origin, reveals the oligomer/polymer nature to be an important prerequisite for photoprotection. Starting from the dimer level, DHICA-derived polymerization products feature ultrafast UV-dissipation with high efficiency, by an excited state quenching mechanism involving solvent mediated intra- and interunit proton transfer via COOH, NH, and OH functionalities. Very efficient UV-dissipation and photoprotection mechanisms are a unique property of DHICA oligomeric structures and appear to be strictly related to the peculiar mode of bonding DHICA via atropisomeric biphenyl-type bondings, inasmuch as the corresponding carboxyl-free structures in 2-linked DHI oligomers can only give rise to long-lived excited states or reactive radical species.[21]

■ CONCLUSIONS

In the present study we have demonstrated that the superior photoprotective properties of black eumelanin pigments are specifically due to the unique photophysical and photochemical behavior of the DHICA-derived oligomeric motifs. The following main conclusions have been drawn:

1. DHICA dimers provide the minimum functional unit for very efficient UV-energy dissipation of eumelanin. Already at the dimer level excited state dissipation is more than 1000 times more efficient than that for a DHICA monomer and very similar to the full polymeric pigment.

dx.doi.org/10.1021/ja501499q | J. Am. Chem. Soc. 2014, 136, 11626−11635

2. This very efficient excited state dissipation results in superior photoprotective properties of black eumelanin pigments, and this work now demonstrates that the protective function is a unique property of coupled DHICA units. Similar carboxyl-free (DHI) structures only exhibit long-lived excited states or radicals.[21]
3. The femtosecond excited state dissipation process is a highly robust solution to eumelanin photoprotection through two mechanistic features,
    a. Independence of dissipation rate of subunit coupling, and
    b. 2-fold paths of excited state decay, governed by intra- and inter- unit ESPT, both occurring on the subpicosecond time scale.
4. Considerable insight into the mechanisms of these two paths has been gained.

The results disclosed herein (a) unveil peculiar excited state deactivation mechanisms which can operate only via interunit mechanisms available specifically to linear DHICA-derived polymeric motifs; (b) highlight skin photoprotection mechanisms that are independent of the π-electron make-up of the individual eumelanin components and depend rather on the interunit bonding patterns within the oligomer/polymer chains; (c) offer a new experimental basis, in addition to free radical scavenging to explain why Nature selected DHICA as a key building block of skin and eye eumelanins despite its nonspontaneous formation and poor chromophore-forming capacity relative to DHI;[76] (d) demonstrate why a highly efficient dopachrome tautomerase activity is essential for skin photoprotection.

Future high level quantum chemistry calculations of DHICA dimers and oligomer potential energy surfaces and the H-bonding network will hopefully clarify the potential energy landscape controlling the reactions and thereby provide a basis for a more quantitative understanding of, e.g., the origin of the observed high rates of ESPT and ESIPT, as well as solvent and deuterium isotope effects on the dynamics. The actual scope and expected impact of these results not only may be related to the rapidly advancing field of melanin biology but also may entail new directions toward the rational engineering of innovative functional materials modeled to natural eumelanins for biomedical applications.[3]

METHODS

Synthesis. Samples were prepared according to procedures reported in literature. Specifically, DHICA was prepared following the procedure in ref 77, dimers were prepared as described in ref 29, and the 4,4′:7′,4″ trimer was prepared as reported in ref 78. Oxidation of DHICA (8.5 mM in 0.1 M pH 7.0 phosphate buffer) was carried out using mushroom tyrosinase (EC 1.14.18.1, 120 mL) under an oxygen stream.[26] After 4 h, oxygenation was stopped and the solution was diluted 25−100-fold with 0.1 M pH 7.0 phosphate buffer. In a PVA-added medium the buffers used were prepared by dissolving PVA in the appropriate weight ratio and warming to prevent cluster formation. Prior to oxidation, buffers were then thermostated at a temperature of 60 °C. When necessary the mixture was treated with a solution of $NaBH_4$ in water (20 mM). The resulting DHICA eumelanin consists of both reduced and oxidized domains (such as in natural eumelanin) in an approximately 1:1 ratio, with the first being predominantly excited at 267−280 nm.[10] For the fluorescence measurements the samples were diluted and absorption spectra were measured. The concentration was set with an absorbance at the excitation wavelength of about 0.2 in a 2 mm cell. Based on the extinction coefficient in ethanol,[26] the concentration for the measurements in both methanol and aqueous buffer is estimated to be ∼0.2 mM. No noticeable changes in the absorption spectrum were observed when the concentration was varied.

Sample Purification (Dimers and Trimer). Efficient removal of all contaminants as well as any emitting species from samples of dimers and trimer (preparation of >98% pure samples, as judged by ^{1}H NMR) was achieved by repeated chromatographic separation. In detail: the appropriate preparation mixture was reduced with an excess of sodium borohydride, acidified with HCl to pH 2, and extracted three times with an equal volume of ethyl acetate. The organic layers were dried over sodium sulfate and evaporated to dryness. The residue was acetylated with acetic anhydride/pyridine 20/1 and chromatographed on preparative HPLC using as the mobile phase 0.4 M formic acid/methanol: gradient from 7/3 to 1/1 over 90 min. The products were collected and carefully evaporated to dryness to give dimers with an over 98% purity grade. Each sample was then chromatographed twice more on preparative HPLC using the isocratic mobile phase 0.4 M formic acid/methanol: 6/4. At each chromatographic step the concentration of the analytes was increased as much as possible in order to reduce the time required for evaporation to dryness.

Steady-State Optical Characterization. Optical absorption spectra were measured using an Agilent spectrophotometer. The contribution from the PVA in the case of the polymer sample is negligible.

Up-Conversion Detection of Time-Resolved Fluorescence. The fluorescence up-conversion measurements were performed with a setup previously described in refs 79 and 80. Briefly, frequency-tripled pulses at 267 nm from a mode-locked Ti-sapphire laser (MIRA, Coherent) were used. The average excitation power was set to 25 mW. The fluorescence from the sample was collected with parabolic mirrors and mixed with the residual fundamental, serving as the gating pulse, in a 0.5 mm type I BBO crystal to generate the sum-frequency light. This was spectrally filtered through a monochromator and detected by a photomultiplier in single-photon counting mode. The spectral resolution was approximately 5 nm. Fluorescence decays were measured by means of a motorized delay stage installed in the optical path of the gating pulse. Parallel and perpendicular excitation−detection polarization conditions were used by adjusting the polarization of the excitation beam with a zero-order half-wave plate. Total fluorescence kinetics were constructed from Ipar(t) + 2 × Iperp(t). The solution was kept in a 1 mm rotating cell equipped with quartz windows. All time-resolved fluorescence measurements were performed at room temperature (20 ± 1 °C), in air. Samples were prepared in order to have an absorption of about 0.2/mm at the excitation wavelength (267 nm), which corresponds to a concentration of ∼0.3 mM for the 4,4′-dimer and 0.2 mM for the 4,7′-dimer in MeOH.[26]

Streak Camera Detection of Time-Resolved Fluorescence. Infrared pulses with a central wavelength of 840 nm, pulse duration of 100 fs, and repetition rate of 82 MHz (Spectra-Physics, Tsunami) were frequently tripled using a harmonic generator (Photop Technologies, Tripler TP-2000B), yielding UV-pulses with a central wavelength of 280 nm. The UV-pulses were focused on the sample using a 100 mm focal length quartz lens. The sample solution was kept under N_2 in a rotating quartz cuvette (optical path length 2 mm, optical density at 280 nm of 0.2, corresponding to concentrations of approximately 0.1 mM[81]). The fluorescence was collected at the magic angle using two 1 in. diameter 50 mm focal length quartz lenses and focused on the input slit of a spectrograph (Chromex), using a grating with 50 lines/mm blazed at 600 nm. The output of the spectrograph was sent into a streak camera setup (Hamamatsu, C6860). The time windows covered were either 2 ns (time range 6) or 200 ps (time range 3). The time resolution at time range 6 and a slit of 100 μm was about 100 ps; at time range 3 and a slit of 40 μm the time resolution was improved to about 5 ps. A time resolution below 5 ps with the necessary narrower time window and slit could not be reached due to too long illumination times, leading to UV-induced chemical degradation of the sample. Experimental data were corrected for background, shading, and curvature. Chemical degradation due to the UV-illumination was excluded on the basis of very similar optical absorption spectra before and after the experiments. In the

dx.doi.org/10.1021/ja501499q | J. Am. Chem. Soc. 2014, 136, 11626−11635

experimental range of 1−5 pJ per pulse, no intensity dependence of the fluorescence dynamics was observed. In addition, no influence of the concentration was observed in the absorbance range 0.1−0.5 at 280 nm in a 2 mm cell. The emission originating from the PVA in the case of the polymer sample was negligible.

Ground State Conformational Calculations. The structures of the 4,4′- and 4,7′-dimers in H_2O in the ground state were created using Shaftenaar's MOLDEN program.[82]

■ ASSOCIATED CONTENT

Supporting Information

Streak camera measurements, and fluorescence steady state spectrum: Figures SI1−SI4. This material is available free of charge via the Internet at http://pubs.acs.org.

■ AUTHOR INFORMATION

Corresponding Author

Villy.Sundstrom@chemphys.lu.se

Present Address

[⊥]Optical Sciences group, MESA+ Institute for Nanotechnology, University of Twente, P.O. Box 217, 7500 AE, The Netherlands.

Notes

The authors declare no competing financial interest.

■ ACKNOWLEDGMENTS

Research performed in Lund was supported by funding from the Wenner−Gren Foundation, the Swedish Energy Agency, the Knut and Wallenberg Foundation and the Swedish Research Council funded Linnaeus program within the Lund Laser Centre and the European Research Council (226136-VISCHEM). A.P. acknowledges support from the European Science Foundation (ESF) for the activity entitled "Ultrafast Structural Dynamics in Physics, Chemistry, Biology and Materials Science", the POLYMED FP7 project "PIRSES-GA-2013-612538" and the "'Laserlab Europe'" integrated infrastructure program at the Lund Laser Centre (Project Number LLC001584). A.P. and M.d'I. also acknowledge financial support by the MIUR (Italy), PRIN 2010−11 (PROxi project). P.-Å. M. would like to acknowledge financial support from the Swedish Research Council (Grant Number VR 2010-5008) and from the Organizing Molecular Matter (OMM) Center of Excellence, Project 239-2009-6794.

■ REFERENCES

(1) Simon, J. D.; Peles, D.; Wakamatsu, K.; Ito, S. *Pigment Cell & Melanoma Research* **2009**, *22*, 563−579.

(2) d'Ischia, M.; Wakamatsu, K.; Napolitano, A.; Briganti, S.; Garcia-Borron, J. C.; Kovacs, D.; Meredith, P.; Pezzella, A.; Picardo, M.; Sarna, T.; Simon, J. D.; Ito, S. *Pigment Cell & Melanoma Research* **2013**, *26*, 616−633.

(3) Panzella, L.; Gentile, G.; D'Errico, G.; Della Vecchia, N. F.; Errico, M. E.; Napolitano, A.; Carfagna, C.; d'Ischia, M. *Angew. Chem., Int. Ed.* **2013**, *52*, 12684−12687.

(4) Panzella, L.; Napolitano, A.; d'Ischia, M. *Pigment Cell & Melanoma Research* **2011**, *24*, 248−249.

(5) Kovacs, D.; Flori, E.; Maresca, V.; Ottaviani, M.; Aspite, N.; Dell'Anna, M. L.; Panzella, L.; Napolitano, A.; Picardo, M.; d'Ischia, M. *J. Invest. Dermatol.* **2012**, *132*, 1196−1205.

(6) Tran, M. L.; Powell, B. J.; Meredith, P. *Biophys. J.* **2006**, *90*, 743−752.

(7) Powell, B. J.; Baruah, T.; Bernstein, N.; Brake, K.; McKenzie, R. H.; Meredith, P.; Pederson, M. R. *J. Chem. Phys.* **2004**, *120*, 8608−8615.

(8) Stark, K. B.; Gallas, J. M.; Zajac, G. W.; Eisner, M.; Golab, J. T. *J. Phys. Chem. B* **2003**, *107*, 3061−3067.

(9) Stark, K. B.; Gallas, J. M.; Zajac, G. W.; Eisner, M.; Golab, J. T. *J. Phys. Chem. B* **2003**, *107*, 11558−11562.

(10) Pezzella, A.; Iadonisi, A.; Valerio, S.; Panzella, L.; Napolitano, A.; Adinolfi, M.; d'Ischia, M. *J. Am. Chem. Soc.* **2009**, *131*, 15270−15275.

(11) Stark, K. B.; Gallas, J. M.; Zajac, G. W.; Golab, J. T.; Gidanian, S.; McIntire, T.; Farmer, P. J. *J. Phys. Chem. B* **2005**, *109*, 1970−1977.

(12) Meredith, P.; Riesz, J. *Photochem. Photobiol.* **2004**, *79*, 211−216.

(13) Nighswander-Rempel, S. P.; Riesz, J.; Gilmore, J.; Bothma, J. P.; Meredith, P. *J. Phys. Chem. B* **2005**, *109*, 20629−20635.

(14) Nighswander-Rempel, S. P. *Biopolymers* **2006**, *82*, 631−637.

(15) Nofsinger, J. B.; Ye, T.; Simon, J. D. *J. Phys. Chem. B* **2001**, *105*, 2864−2866.

(16) Riesz, J.; Sarna, T.; Meredith, P. *J. Phys. Chem. B* **2006**, *110*, 13985−13990.

(17) Ye, T.; Simon, J. D. *J. Phys. Chem. B* **2003**, *107*, 11240−11244.

(18) Gauden, M.; Pezzella, A.; Panzella, L.; Neves-Petersen, M. T.; Skovsen, E.; Petersen, S. B.; Mullen, K. M.; Napolitano, A.; d'Ischia, M.; Sundstrom, V. *J. Am. Chem. Soc.* **2008**, *130*, 17038−17043.

(19) Huijser, A.; Pezzella, A.; Hannestad, J. K.; Panzella, L.; Napolitano, A.; d'Ischia, M.; Sundstrom, V. *ChemPhysChem* **2010**, *11*, 2424−2431.

(20) Corani, A.; Pezzella, A.; Pascher, T.; Gustavsson, T.; Markovitsi, D.; Huisjer, A.; d'Ischia, M.; Sundstrom, V. *J. Phys. Chem. Lett.* **2013**, *4*, 1383−1388.

(21) Corani, A.; Huijser, A.; Iadonisi, A.; Pezzella, A.; Sundstom, V.; d'Ischia, M. *J. Phys. Chem. B* **2012**, *116*, 13151−13158.

(22) d'Ischia, M.; Napolitano, A.; Pezzella, A.; Meredith, P.; Sarna, T. *Angew. Chem., Int. Ed.* **2009**, *48*, 3914−3921.

(23) Ascione, L.; Pezezella, A.; Ambrogi, V.; Carfagna, C.; d'Ischia, M. *Photochemistry and Photobiology* **2013**, *89*, 314−318.

(24) Charkoudian, L. K.; Franz, K. J. *Inorg. Chem.* **2006**, *45*, 3657−3664.

(25) Olsen, S.; Riesz, J.; Mahadevan, I.; Coutts, A.; Bothma, J. P.; Powell, B. J.; McKenzie, R. H.; Smith, S. C.; Meredith, P. *J. Am. Chem. Soc.* **2007**, *129*, 6672−6673.

(26) Pezzella, A.; Napolitano, A.; dIschia, M.; Prota, G. *Tetrahedron* **1996**, *52*, 7913−7920.

(27) Pezzella, A.; dIschia, M.; Napolitano, A.; Palumbo, A.; Prota, G. *Tetrahedron* **1997**, *53*, 8281−8286.

(28) Huijser, A.; Rode, M. F.; Corani, A.; Sobolewski, A. L.; Sundstrom, V. *Phys. Chem. Chem. Phys.* **2012**, *14*, 2078−2086.

(29) Pezzella, A.; Vogna, D.; Prota, G. *Tetrahedron: Asymmetry* **2003**, *14*, 1133−1140.

(30) Huijser, A.; Pezzella, A.; Sundstrom, V. *Phys. Chem. Chem. Phys.* **2011**, *13*, 9119−9127.

(31) Karton-Lifshin, N.; Presiado, I.; Erez, Y.; Gepshtein, R.; Shabat, D.; Huppert, D. *J. Phys. Chem. A* **2012**, *116*, 85−92.

(32) Presiado, I.; Erez, Y.; Huppert, D. *J. Phys. Chem. A* **2010**, *114*, 9471−9479.

(33) Sakota, K.; Sekiya, H. *J. Phys. Chem. A* **2005**, *109*, 2722−2727.

(34) Gould, E. A.; Popov, A. V.; Tolbert, L. M.; Presiado, I.; Erez, Y.; Huppert, D.; Solntsev, K. M. *Phys. Chem. Chem. Phys.* **2012**, *14*, 8964−8973.

(35) Simkovitch, R.; Shomer, S.; Gepshtein, R.; Shabat, D.; Huppert, D. *J. Phys. Chem. A* **2013**, *117*, 3925−3934.

(36) Simkovitch, R.; Karton-Lifshin, N.; Shomer, S.; Shabat, D.; Huppert, D. *J. Phys. Chem. A* **2013**, *117*, 3405−3413.

(37) Schriever, C.; Lochbrunner, S.; Ofial, A. R.; Riedle, E. *Chem. Phys. Lett.* **2011**, *503*, 61−65.

(38) Brucker, G. A.; Swinney, T. C.; Kelley, D. F. *J. Phys. Chem.* **1991**, *95*, 3190−3195.

(39) Frey, W.; Laermer, F.; Elsaesser, T. *J. Phys. Chem.* **1991**, *95*, 10391−10395.

(40) Saltiel, J.; Waller, A. S.; Sears, D. F. *J. Photochem. Photobiol., A* **1992**, *65*, 29−40.

(41) Sension, R. J.; Repinec, S. T.; Szarka, A. Z.; Hochstrasser, R. M. *J. Chem. Phys.* **1993**, *98*, 6291−6315.

(42) Akesson, E.; Bergstrom, H.; Sundstrom, V.; Gillbro, T. *Chem. Phys. Lett.* **1986**, *126*, 385−393.

(43) Akesson, E.; Sundstrom, V.; Gillbro, T. *Chem. Phys.* **1986**, *106*, 269−280.
(44) Sundstrom, V.; Gillbro, T. *J. Chem. Phys.* **1984**, *81*, 3463−3474.
(45) Sundstrom, V.; Gillbro, T.; Gadonas, R. A.; Piskarskas, A. *J. Chem. Phys.* **1988**, *89*, 2754−2762.
(46) Van Amerongen, H.; Valkunas, L.; Van Gromdelle, R. *Photosynthetic Excitons*: World Scientific: 2010.
(47) Marguet, S.; Markovitsi, D.; Millie, P.; Sigal, H.; Kumar, S. *J. Phys. Chem. B* **1998**, *102*, 4697−4710.
(48) Sundstrom, V.; Pullerits, T.; van Grondelle, R. *J. Phys. Chem. B* **1999**, *103*, 2327−2346.
(49) Kasha, M.; Rawls, H. R.; Ashraf El-Bayoumi, M. *The Exciton Model in Molecular Spectroscopy; Pure Appl. Chem.* **1965**, 371−392.
(50) Ottiger, P.; Leutwyler, S. *Chimia* **2011**, *65*, 228−230.
(51) Ottiger, P.; Leutwyler, S.; Koppel, H. *J. Chem. Phys.* **2012**, *136*, 174308.
(52) Tolbert, L. M.; Solntsev, K. M. *Acc. Chem. Res.* **2002**, *35*, 19−27.
(53) Agmon, N.; Huppert, D.; Masad, A.; Pines, E. *J. Phys. Chem.* **1991**, *95*, 10407−10413.
(54) Ando, K.; Hynes, J. T. *J. Mol. Liq.* **1995**, *64*, 25−37.
(55) Krishnan, R.; Lee, J.; Robinson, G. W. *J. Phys. Chem.* **1990**, *94*, 6365−6367.
(56) Pines, E.; Fleming, G. R. *J. Phys. Chem.* **1991**, *95*, 10448−10457.
(57) Agmon, N. *J. Phys. Chem. A* **2005**, *109*, 13−35.
(58) Arnaut, L. G.; Formosinho, S. J. *J. Photochem. Photobiol., A* **1993**, *75*, 1−20.
(59) Sobolewski, A. L.; Domcke, W. *Phys. Chem. Chem. Phys.* **2006**, *8*, 3410−3417.
(60) Sobolewski, A. L.; Domcke, W.; Hattig, C. *J. Phys. Chem. A* **2006**, *110*, 6301−6306.
(61) Sobolewski, A. L.; Domcke, W. *ChemPhysChem* **2007**, *8*, 756−762.
(62) Cohen, B.; Alvarez, C. M.; Carmona, N. A.; Organero, J. A.; Douhal, A. *J. Phys. Chem. B* **2011**, *115*, 7637−7647.
(63) Erez, Y.; Huppert, D. *J. Phys. Chem. A* **2010**, *114*, 8075−8082.
(64) Erez, Y.; Gepshtein, R.; Presiado, I.; Trujillo, K.; Kallio, K.; Remington, S. J.; Huppert, D. *J. Phys. Chem. B* **2011**, *115*, 11776−11785.
(65) Kennis, J. T. M.; Larsen, D. S.; van Stokkum, I. H. M.; Vengris, M.; van Thor, J. J.; van Grondelle, R. *Proc. Natl. Acad. Sci. U.S.A.* **2004**, *101*, 17988−17993.
(66) Zimmer, M. *Chem. Rev.* **2002**, *102*, 759−781.
(67) Tolbert, L. M.; Harvey, L. C.; Lum, R. C. *J. Phys. Chem.* **1993**, *97*, 13335−13340.
(68) Manca, C.; Tanner, C.; Leutwyler, S. *Int. Rev. Phys. Chem.* **2005**, *24*, 457−488.
(69) Tanner, C.; Manca, C.; Leutwyler, S. *Chimia* **2004**, *58*, 234−236.
(70) Harris, C. M.; Selinger, B. K. *J. Phys. Chem.* **1980**, *84*, 1366−1371.
(71) Pines, E.; Fleming, G. R. *Chem. Phys.* **1994**, *183*, 393−402.
(72) Presiado, I.; Karton-Lifshin, N.; Erez, Y.; Gepshtein, R.; Shabat, D.; Huppert, D. *J. Phys. Chem. A* **2012**, *116*, 7353−7363.
(73) Borgis, D.; Hynes, J. T. *J. Chem. Phys.* **1991**, *94*, 3619−3628.
(74) Borgis, D.; Hynes, J. T. *J. Phys. Chem.* **1996**, *100*, 1118−1128.
(75) Borgis, D. C.; Lee, S. Y.; Hynes, J. T. *Chem. Phys. Lett.* **1989**, *162*, 19−26.
(76) Tsukamoto, K.; Palumbo, A.; dIschia, M.; Hearing, V. J.; Prota, G. *Biochem. J.* **1992**, *286*, 491−495.
(77) Edge, R.; d'Ischia, M.; Land, E. J.; Napolitano, A.; Navaratnam, S.; Panzella, L.; Pezzella, A.; Ramsden, C. A.; Riley, P. A. *Pigment Cell Research* **2006**, *19*, 443−450.
(78) Pezzella, A.; Vogna, D.; Prota, G. *Tetrahedron* **2002**, *58*, 3681−3687.
(79) Gustavsson, T.; Sharonov, A.; Markovitsi, D. *Chem. Phys. Lett.* **2002**, *351*, 195−200.
(80) Gustavsson, T.; Improta, R.; Banyasz, A.; Vaya, I.; Markovitsi, D. *J. Photochem. Photobiol., A* **2012**, *234*, 37−43.
(81) Pezzella, A.; Panzella, L.; Crescenzi, O.; Napolitano, A.; Navaratnam, S.; Edge, R.; Land, E. J.; Barone, V.; d'Ischia, M. *J. Org. Chem.* **2009**, *74*, 3727−3734.
(82) Schaftenaar, G.; Noordik, J. H. *J. Comput.-Aided Mol. Des.* **2000**, *14*, 123−134.
(83) Jimenez, R.; Fleming, G. R.; Kumar, P. V.; Maroncelli, M. *Nature* **1994**, *369*, 471−473.